

RESEARCH

Open Access



NGEF is a potential prognostic biomarker and could serve as an indicator for immunotherapy and chemotherapy in lung adenocarcinoma

Xin Chen^{1*}, Tao Zhang^{2†}, Yan-qiu He^{1†}, Ti-wei Miao¹, Jie Yin³, Qian Ding¹, Mei Yang¹, Fang-ying Chen⁴, Hong-ping Zeng¹, Jie Liu¹ and Qi Zhu¹

Abstract

Background Neuronal guanine nucleotide exchange factor (NGEF) plays a key role in several cancers; however, its role in lung adenocarcinoma (LUAD) remains unclear. The aim of this study was to evaluate the efficacy of NGEF as a prognostic biomarker and potential therapeutic target for LUAD.

Methods NGEF expression data for multiple cancers and LUAD were downloaded from multiple databases. The high- and low-NGEF expression groups were constructed based on median NGEF expression in LUAD samples, and then performed Kaplan–Meier survival analysis. Differentially expressed genes (DEGs) from the two NGEF expression groups were screened and applied to construct a protein-protein interaction network. The primary pathways were obtained using gene set enrichment analysis. The associations between NGEF expression and clinical characteristics, immune infiltration, immune checkpoint inhibitors (ICIs), sensitivity to chemotherapy, and tumor mutation burden (TMB) were investigated using R. Levels of NGEF expression in the lung tissue was validated using single-cell RNA sequencing, quantitative polymerase chain reaction (qPCR), immunohistochemical staining, and western blot analysis.

Results The expression of NGEF mRNA was upregulated in multiple cancers. mRNA and protein expression levels of NGEF were higher in patients with LUAD than in controls, as validated using qPCR and western blot. High NGEF expression was an independent prognostic factor for LUAD and was associated with advanced tumor stage, large tumor size, more lymph node metastasis, and worse overall survival (OS). A total of 182 overlapping DEGs were screened between The Cancer Genome Atlas and GSE31210, among which the top 20 hub genes were identified. NGEF expression was mainly enriched in the pathways of apoptosis, cell cycle, and DNA replication. Moreover, elevated NGEF expression were associated with a high fraction of activated memory CD4⁺ T cells and M₀ macrophages; elevated expression levels of the ICIs: programmed cell death 1 and programmed cell death 1 ligand

[†]Xin Chen, Tao Zhang, and Yan-qiu He should be considered as co-first authors.

*Correspondence:
Xin Chen
4651740@qq.com

Full list of author information is available at the end of the article



© The Author(s) 2024. **Open Access** This article is licensed under a Creative Commons Attribution 4.0 International License, which permits use, sharing, adaptation, distribution and reproduction in any medium or format, as long as you give appropriate credit to the original author(s) and the source, provide a link to the Creative Commons licence, and indicate if changes were made. The images or other third party material in this article are included in the article's Creative Commons licence, unless indicated otherwise in a credit line to the material. If material is not included in the article's Creative Commons licence and your intended use is not permitted by statutory regulation or exceeds the permitted use, you will need to obtain permission directly from the copyright holder. To view a copy of this licence, visit <http://creativecommons.org/licenses/by/4.0/>. The Creative Commons Public Domain Dedication waiver (<http://creativecommons.org/publicdomain/zero/1.0/>) applies to the data made available in this article, unless otherwise stated in a credit line to the data.

1 expression; higher TMB; and better sensitivity to bortezomib, docetaxel, paclitaxel, and parthenolide, but less sensitivity to axitinib and metformin.

Conclusion NGEF expression is upregulated in LUAD and is significantly associated with tumor stages, OS probability, immune infiltration, immunotherapy response, and chemotherapy response. NGEF may be a potential diagnostic and prognostic biomarker and therapeutic target in LUAD.

Keywords Neuronal guanine nucleotide exchange factor, Lung adenocarcinoma, Prognosis, Immune infiltration, Immunotherapy, Chemotherapy

Introduction

Lung cancer accounts for approximately 18% of the deaths caused by cancer worldwide [1], and its largest subgroup is lung adenocarcinoma (LUAD) [2]. LUAD is primarily located in distal lung and is difficult to diagnose through bronchoscopy, thereby posing a significant challenge on diagnosis [3]. Non-small cell lung cancer (NSCLC) is often not detected until they reach stages IIIB and IV; therefore, they have no opportunity for surgery [4]. Recently, a CT-guided thoracic core-needle biopsy shows an improved diagnostic accuracy for LUAD [5]. Although there has been a constant progress in disease diagnosis and targeted and immune therapies for LUAD patients over the past decades, the average 5-year overall survival (OS) probability maintains not more than 20% [6, 7]. Therefore, identifying effective biomarkers for predicting patient prognosis and/or therapeutic response is important for patients with LUAD.

Several biomarkers have been explored to diagnose LUAD and predict its prognosis. For example, the molecule CD1b (CD1B) is a novel prognostic biomarker in LUAD and related to its tumor mutation burden (TMB) as well as antitumor immunity [8]. Tumor protein D52-like 2 (TPD52L2) is an oncogene in LUAD, and associates with prognosis, and immune infiltration [9]. Mini-chromosome maintenance 5 (MCM5) expression is related to OS probability and clinical parameters, including TNM stage, pathological stage, and smoking status, in LUAD [10]. High eukaryotic initiation factor 3 (eIF3D) expression is independently associated with lower OS probability in LUAD [11]. Programmed death-ligand 1 (PD-L1) expression was positively correlated with the emergence of invasiveness and pathological subtype or biological behavior of early-stage lung adenocarcinoma [12]. However, these biomarkers are currently insufficient for the diagnosis and prognosis prediction of LUAD because of their complex molecular mechanisms and disease heterogeneity. For example, a joint analysis of transcriptome and proteome data shows that LUAD can be clustered into four novel subtypes with distinct molecular characteristics [13]. Therefore, new biomarkers need to be explored to better understand the complex molecular mechanisms, facilitate novel therapeutic methods, and improve the prognosis of LUAD patients.

Neuronal guanine nucleotide exchange factor (NGEF, also known as Ephexin1) is a member of a subfamily of the Dbl family of guanine nucleotide exchange factors (GEFs), and acts as a direct link between Eph receptors and the Rho-family of GTPases [14–16]. It was localized in mouse chromosome 1 and human chromosome 2q37 [16]. NGEF is mainly correlated with myopia and obesity-related diseases [17, 18]. However, several reports have demonstrated the involvement of NGEF in cancer. Wang et al. demonstrated that NGEF expression was upregulated in patients with malignant thyroid nodules; therefore, they reported NGEF as a potential diagnostic biomarker [19]. In addition, Han et al. showed that levels of NGEF expression were risen in patients with papillary thyroid cancer and were associated with a lower OS [20]. Thus, NGEF may act as an oncogene and may be associated with cancer prognosis. However, the diagnostic and prognostic importance of NGEF in patients with LUAD remains unclear. In this context, the current study explored the diagnostic and prognostic importance of NGEF in patients with LUAD.

In our study, NGEF expression, methylation, and gene mutation data for LUAD were comprehensively analyzed with the Gene Expression Profiling Interactive Analysis 2 (GEPIA2), The Cancer Genome Atlas (TCGA), and Gene Expression Omnibus (GEO) databases. The expression levels of NGEF mRNA were compared between LUAD and control samples. The results of bioinformatic analyses were validated by using quantitative polymerase chain reaction (qPCR), immunohistochemical (IHC) staining, single-cell RNA sequencing (scRNA-seq), and western blot analysis. The potential prognostic value of NGEF in LUAD was assessed using Kaplan–Meier survival curve, multivariable Cox regression analyses, and a nomogram. Differentially expressed genes (DEGs) from the two NGEF expression groups were screened and used to construct a protein-protein interaction (PPI) network. The primary pathways between the two NGEF expression groups were identified with gene set enrichment analysis. The R was used to evaluate the associations of NGEF expression with tumor stage, immune infiltration, immune checkpoint inhibitors (ICIs), TMB, and sensitivity to chemotherapy.

Methods and materials

Data collection and processing

The NGEF mRNA expression data for the most common cancers in China, such as LUAD (483 cancer tissues and 347 normal tissues), lung squamous cell carcinoma (LUSC, 486 cancer tissues and 338 normal tissues), stomach adenocarcinoma (STAD, 408 cancer tissues and 211 normal tissues), liver hepatocellular carcinoma (LIHC, 369 cancer tissues and 160 normal tissues), colon adenocarcinoma (COAD, 275 cancer tissues and 349 normal tissues), rectum adenocarcinoma (READ, 92 cancer tissues and 318 normal tissues), breast invasive carcinoma (BRCA, 1085 cancer tissues and 291 normal tissues), and thyroid carcinoma (THCA, 512 cancer tissues, and 337 normal tissues) were downloaded from the GEPIA2 database (<http://gepia2.cancer-pku.cn/#index>) [21, 22]. The mRNA expression data in the GEPIA2 database were acquired from TCGA and GTEx databases. In addition, 535 LUAD tissues and 59 normal tissues with mRNA expression data (FPKM format), 437 LUAD tissues and 29 normal tissues with methylation data, 560 LUAD tissues with mutation data, and 522 LUAD tissues with clinical characteristics data were downloaded from TCGA-GDC database (<https://portal.gdc.cancer.gov/>) [23, 24]. Additionally, 226 LUAD tissues and 20 normal tissues with mRNA expression data and 226 LUAD tissues with clinical characteristics data were obtained from the GEO database (<https://www.ncbi.nlm.nih.gov/gds/>) [25, 26]. GSE31210 dataset was generated by GPL570 [HG-U133_Plus_2] Affymetrix Human Genome U133 Plus 2.0 Array. Levels of NGEF expression were compared between LUAD samples and control samples in both TCGA and GSE31210 datasets. The ROC curve analysis was performed using GraphPad Prism (version 7.00), and the area under the curve (AUC) value, cut-off value, sensitivity, and specificity were calculated. Patients with LUAD who had complete follow-up information were enrolled for further analysis.

Associations of NGEF expression levels with clinical characteristics

The high- or low-NGEF expression groups were constructed using all patients according to the median NGEF expression values obtained using R (version 4.0.2). Kaplan–Meier survival analysis was performed between the two NGEF expression groups and compared by the log-rank test using “limma” packages in R. The survival curve was plotted using “ggpubr” packages. Levels of NGEF expression were compared among different age groups, gender groups, Union for International Cancer Control (UICC) stages, T stages, N stages, and M stages. Univariate and multivariate Cox regression analyses were performed to screen independent prognostic factors for LUAD using “survival” packages in R and drew forest

plot. P -value < 0.05 was seen as statistical significance, and the hazard ratio (HR) was estimated.

Construction of nomogram and calibration plots

A nomogram can be constructed using multiple parameters, including clinical characteristics and RNA sequencing data [27, 28]; thus, nomograms can better reflect prognosis and guide individualized therapy. A nomogram was established including UICC stage, and NGEF values using the “survival,” “regplot,” and “rms” packages in R. Difference of actual and predicted OS probability at 1, 3, and 5 years was evaluated using calibration plots of the nomogram.

Identification of DEGs

The DEGs between the two NGEF expression groups were identified in TCGA and GSE31210 using the “limma” package in R based on $|\log_2$ fold change (FC)| ≥ 0.5 and false discovery rate (FDR) < 0.05 . Heatmaps were drawn in TCGA and GSE31210 using the “pheatmap” packages in R. The overlapping DEGs were screened between TCGA and GSE31210 database using “Venn” packages in R.

Establishment of PPI network and identification of hub genes

The STRING (<https://string-db.org>, version 11.0) is an online database applied to establish a PPI network of genes based on the known and predicted targets [29]. The PPI network was generated by utilizing the overlapping DEGs in the STRING database and then imported into Cytoscape (version 3.7.1) to identify the top 20 hub genes.

Gene set enrichment analysis (GSEA) of NGEF

GSEA can be applied to determine whether a previously defined set of genes show statistical significance between two different groups [30]. According to the median NGEF expression values in LUAD, the high- and low-NGEF expression groups (NGEF.cls) and mRNA expression values (NGEF.gct) were obtained using Strawberry Perl (version 5.34.1). GSEA (version 4.0.3) was obtained from GSEA online website (<http://www.gsea-msigdb.org/gsea/index.jsp>). Pathway analyses between the two NGEF expression groups were run using GSEA using “c2.cp.kegg.v7.5.1.symbols.gmt”, and the phenotype label was “H-versus-L” and the standard of permutations was 1,000. A nominal P -value of < 0.05 and FDR of < 0.05 was considered statistical significance.

Methylation and tumor mutation burden analyses

Methylation data and matrix for LUAD were obtained using Strawberry Perl. The Mann-Whitney test was used to evaluate difference in methylation between the two

NGEF-expression groups. The data for gene mutation were downloaded from TCGA database. Gene mutation frequencies in the different NGEF expression groups were estimated utilizing “maftools” packages in R. The correlations between NGEF mRNA expression levels and TMB were evaluated using the Mann-Whitney test and Spearman rank correlation analysis. Kaplan–Meier survival analysis was performed between the high-NGEF expression+high TMB and low-NGEF expression+low TMB groups and compared using log-rank test with R.

Association of NGEF with immune infiltration and immunotherapy

Tumor micro-environment score was obtained by “limma” and “e1071” packages in R according to mRNA expression matrix of LUAD. Violin plot was applied to compare and display different immune infiltration profiles between the high- and low-NGEF expression groups using “vioplot” packages in R. In addition, the associations between immune infiltration levels and NGEF expression levels were evaluated using R. Comparisons were performed using Spearman rank correlation analysis, and *P*-value of <0.05 and $|r| > 0.1$ were statistical significance. The mRNA levels of ICIs (PD1 and PDL1) were compared between the different NGEF groups, and correlations were evaluated using Spearman rank correlation analysis.

Association of NGEF with sensitivity to chemotherapy

Six chemotherapy drugs, including bortezomib [31, 32], docetaxel [33, 34], paclitaxel [35, 36], parthenolide [37, 38], axitinib [39–41], and metformin [42, 43], had shown their antitumor effects in lung cancer. The sensitivity to chemotherapy was calculated and evaluated between the two NGEF-expression groups using “pRRophetic” packages in R, and the half inhibitory concentration (IC50) was viewed as a reference standard of drug sensitivity.

RNA extraction and quantitative PCR validation

Lung tissues (30 controls, 30 LUAD) were obtained from Zigong First People’s Hospital. The E.Z.N.A. HP Total RNA Kit (Omega, GA, USA) was used to extract total RNA, and then synthesized cDNA using the PrimeScript™ RT Reagent Kit (Takara, Japan) according to the instructions. The iQ™ SYBR Green Supermix (Bio-Rad) was applied to perform qPCR following the protocol. Beta-actin Ct value (endogenous reference) was used to normalize the relative gene expression levels, using the $2^{-\Delta\Delta C_t}$ relative quantification method. The quantitative PCR primers used were as follows:

NGEF-forward: 5'-TCCTGGACAAGACTGACGAC-3'.

NGEF-reverse: 5'-TCCATCTTGTGGACACGGAA-3'.

Beta-actin-forward: 5'-CCACGAACTACCTTCAACTCC-3'.

Beta-actin-reverse: 5'-GTGATCTCCTTCTGCATCTGT-3'.

Single-cell RNA sequencing analysis

Single-cell RNA sequencing data for lung cancer, NSCLC, and LUAD were obtained from the GEO database. The inclusion criteria for the datasets were: (1) human samples, (2) LUAD, and (3) different cell types. The raw data and phenotype information of the selective dataset were obtained from the above database. The relative expression levels of NGEF were compared among different cell types.

Total protein extraction and western blot analysis

Protein phosphatase inhibitor cocktail (Applygen Technologies, China), phenylmethylsulfonyl fluoride (PMSF) (Beyotime Biotechnology, China), and radioimmunoprecipitation assay (RIPA) buffer (Beyotime Biotechnology, China) were applied to extract total protein from cancer and control tissues of LUAD, and then determined its concentration via the BCA Protein Assay Kit (Thermo, USA). The sodium dodecyl sulfate-polyacrylamide gel electrophoresis with 10% running gel was used to load protein and then transferred onto a polyvinylidene fluoride (PVDF) membrane (Merck, USA). The raw PVDF membrane have been cropped according to the molecular weight and the top and bottom two markers of NGEF and Beta-actin membranes were retained. The cropped PVDF membranes were then incubated with primary antibodies against NGEF (1:1000, Abcam, ab157593, UK) or Beta-actin (1:2000, Proteintech, China) overnight at 4°C after blocking using 5% bovine serum albumin for 2 h. The PVDF membranes were washed with Tris-buffered saline (TBS-T) five times for five minutes, incubated with secondary antibody (1:5,000, boster, China) for 2 h, and washed again. Subsequently, NGEF protein expression levels were determined.

Immunohistochemical (IHC) staining

IHC staining of NGEF in normal lung tissues and LUAD tissues was downloaded from the Human Protein Atlas database (<https://www.proteinatlas.org/>) [44].

Statistical analysis

GraphPad Prism (version 7.00) and R were used to perform statistical analyses and drawing all the figures. According to the nonparametric distribution, levels of gene relative expression were displayed as median (interquartile range), and statistical analysis were performed

using the Mann–Whitney test. A P -value of <0.05 was considered statistical significance.

Results

Increased levels of NGEF expression in multiple cancers

A flowchart of this study is demonstrated in Fig. 1. The data from the GEPIA2 database reported that NGEF expression levels were upregulated in LUAD, LUSC, COAD, READ, and THCA ($P<0.05$, Fig. 2A). Lung cancer is primary reason for the deaths caused by cancer [1]. LUAD is the largest subgroup of lung cancers [2]. Therefore, LUAD was selected for further analyses. 490 patients from TCGA and 226 patients from GSE31210 were included. Table 1 shows baseline information of all patients enrolled. The patients with LUAD presented an increase in levels of NGEF expression in comparison with controls in TCGA database ($P<0.001$, Fig. 2B). The AUC value with 95% CIs for NGEF levels in the lungs for the diagnosis of LUAD was 0.872 (0.834–0.910), with a cut-off value of 0.3761, sensitivity of 81.31%, and specificity of 83.05% based on Youden's index (Fig. 2C). Moreover, NGEF expression levels were risen in LUAD compared with controls in GSE31210 ($P<0.001$, Fig. 2E), and its AUC value for the diagnosis of cancer was 0.820 (0.736–0.904) (Fig. 2F). Thus, NGEF is a diagnostic biomarker for LUAD.

Increased NGEF expression in LUAD was correlated with prognosis and clinical parameters

We next investigated the prognostic value of NGEF in LUAD. Kaplan–Meier survival curve demonstrated that the high NGEF expression levels experienced a shorter OS than the low NGEF expression levels in LUAD from TCGA database ($P<0.001$, Fig. 2D) and GSE31210 datasets ($P<0.001$, Fig. 2G). NGEF expression levels were positively correlated with UICC stage ($P=0.042$, Fig. 3A), tumor size (>3 cm, $P=0.020$, Fig. 3B), and lymph node metastasis (number ≥ 1 , $P<0.001$, Fig. 3C). However, there was not a statistical significance in different M stages ($P=0.682$), age groups ($P=0.887$), or gender groups ($P=0.685$) (Fig. 3D–F). The UICC stage ($P<0.001$; hazard ratio, HR: 1.674) and NGEF ($P<0.001$; HR: 1.060) were associated with prognosis in univariate Cox regression analysis (Fig. 3G). The UICC stage ($P<0.001$, HR: 1.680) and NGEF ($P=0.015$, HR: 1.049) were independently associated with prognosis in multivariate Cox regression analysis (Fig. 3H). Thus, the above findings show that NGEF is an independently prognostic biomarker for LUAD.

Construction of nomogram and calibration plots

To further study prognostic value of NGEF in LUAD, a nomogram was drawn using the UICC stage and NGEF expression levels, and the estimated OS probability at 1, 3, and 5 years can be calculated by this nomogram

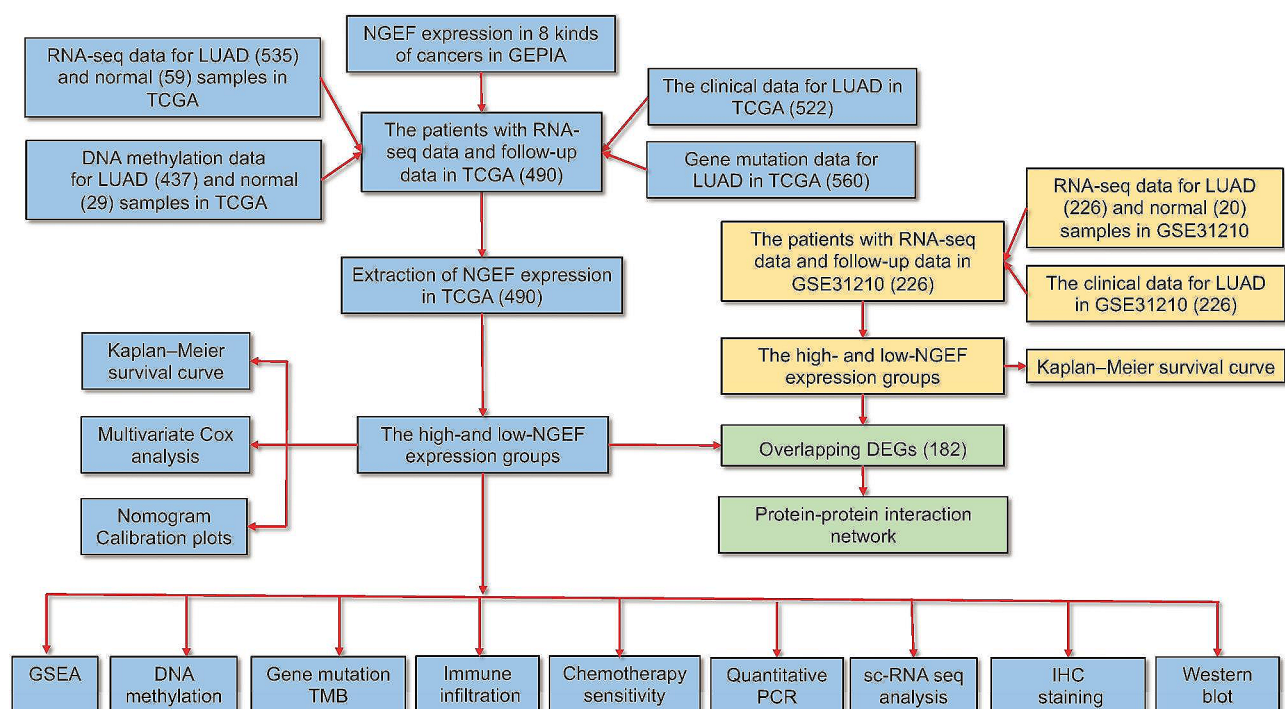


Fig. 1 Study flowchart

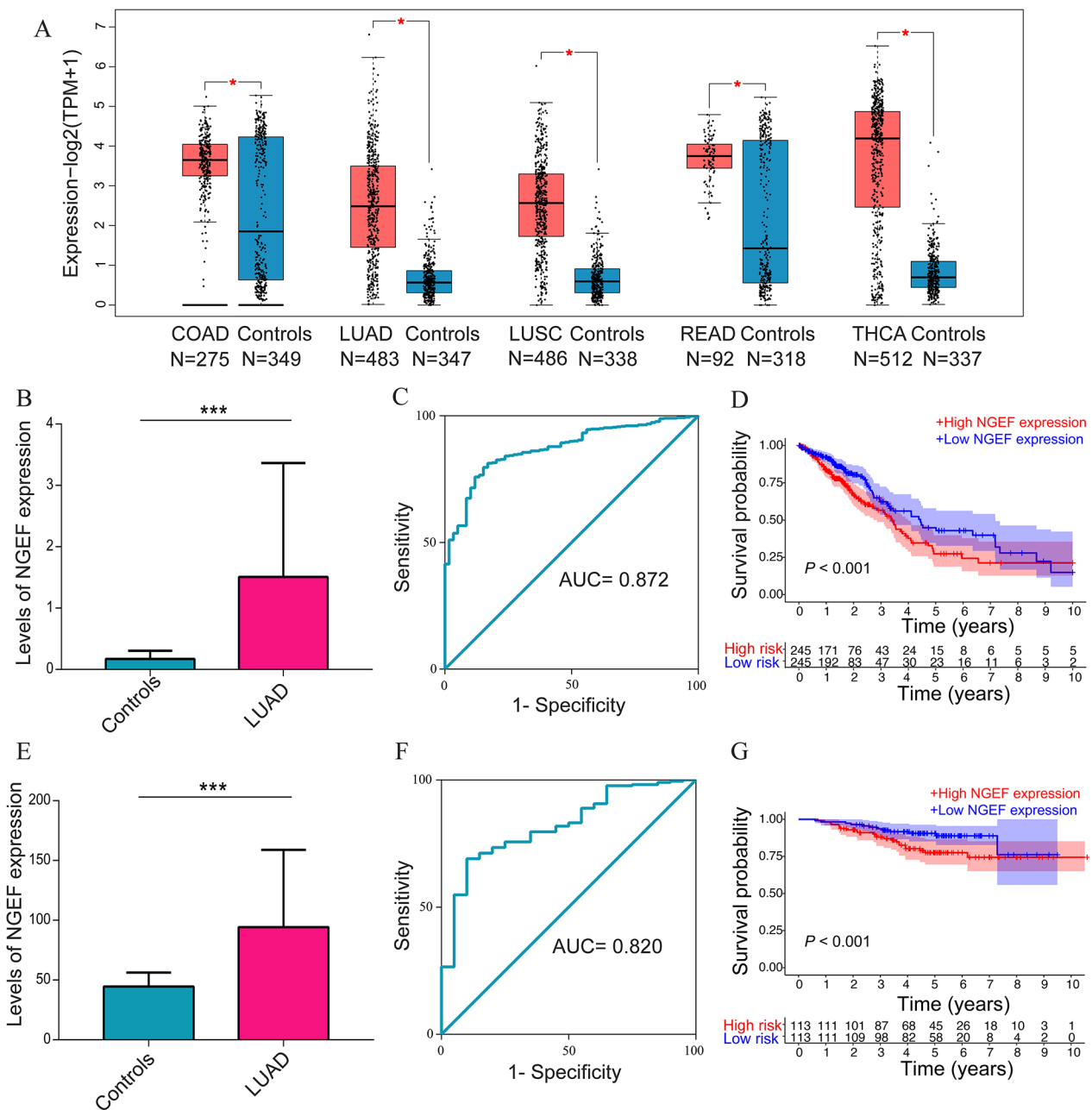


Fig. 2 Diagnostic and prognostic value of NGEF. **(A)** Levels of NGEF expression in five tumor types in the GEPIA2. **(B, E)** Levels of NGEF expression in LUAD in TCGA and GSE31210. **(C, F)** Receiver operating characteristic curve analysis in TCGA and GSE31210. **(D, G)** Kaplan–Meier survival curve analysis in TCGA and GSE31210. NGEF, neuronal guanine nucleotide exchange factor; GEPIA2, Gene Expression Profiling Interactive Analysis 2; TCGA, The Cancer Genome Atlas, COAD, colon adenocarcinoma; LUAD, lung adenocarcinoma; LUSC, lung squamous cell carcinoma; READ, rectum adenocarcinoma; THCA, thyroid carcinoma; N, sample size. * $P < 0.05$, ** $P < 0.01$, *** $P < 0.001$

(Fig. 3I). Calibration plots of the nomogram proved its high predictive accuracy (Fig. 3J).

Identification of DEGs and hub genes

The differentially expressed analysis was performed, and a total of 1,099 DEGs (766 up-regulated and 333 down-regulated genes) were obtained using the “limma” packages

in R when comparing the high-NGEF expression group with the low-NGEF expression group in TCGA ($|\log_2 FC| \geq 0.5$ and $FDR < 0.05$, Table S1). Moreover, 968 DEGs (529 up-regulated and 439 down-regulated genes) were screened in GSE31210 ($|\log_2 FC| \geq 0.5$ and $FDR < 0.05$, Table S2). Heatmaps created using TCGA and GSE31210 are illustrated in Fig. 4A and B, respectively. A total of

Table 1 Clinical features of patients with LUAD from TCGA and GSE31210

Clinical characteristics	TCGA (490)	GSE31210 (226)
Age (years)		
>=65	219 (44.69%)	62 (27.43%)
<65	271 (55.31%)	164 (72.57%)
unknown	0	0
Gender		
Male	224 (45.71%)	105 (46.46%)
Female	266 (54.29%)	121 (53.54%)
unknown	0	0
UICC stages		
Stage I-II	378 (77.14%)	226 (100%)
Stage III-IV	104 (21.22%)	/
unknown	8 (1.63%)	/
T stages		
T1	166 (33.88%)	/
T2-4	321 (66.51%)	/
unknown	3 (0.61%)	/
N stages		
N0	317 (64.69%)	/
N1-3	162 (33.06%)	/
unknown	11 (2.24%)	/
M stages		
M0	322 (65.71%)	/
M1	24 (4.90%)	/
unknown	144 (29.39%)	/

182 overlapping DEGs were screened between TCGA and GSE31210 datasets using the “Venn” packages (Fig. 4C). A PPI network was generated using 182 overlapping DEGs in the STRING database (Figure S1) and was visualized in the Cytoscape. The top 20 hub genes were screened using “Degree” in the Cytoscape (Fig. 4D, and Table 2), among which the top five genes were SPP1, SOX9, GRIA1, IBSP, and PLAU.

GSEA

To identify potential pathways between the two NGEF expression groups, GSEA was run. The findings showed that gene sets were primarily enriched in apoptosis, cell cycle, chemokine signaling pathway, and DNA replication in the high-NGEF expression group in LUAD (FDR<0.05, nominal P <0.05; Fig. 4E-H). Thus, we can infer that various pathways are enriched in the high-NGEF expression group.

Increased NGEF expression was associated with higher TMB but not with methylation levels

Since DNA methylation controls gene expression and thus influence prognosis and TMB is also correlated with prognosis, methylation levels and tumor mutation burden were analyzed between the two NGEF expression groups. Methylation levels of NGEF between the two groups did not reach a statistical significance (Fig. 5A).

The high-NGEF expression group had higher gene mutation frequencies compared to low-NGEF expression group, and the top three mutated genes were TP53, TTN, and MUC16 in both NGEF expression groups (Fig. 5B-C). TMB was risen in the high-NGEF expression group compared with the low-NGEF expression group ($P=0.041$, Fig. 5D), and the correlation of NGEF mRNA expression levels with TMB was at the border of a statistical difference ($P=0.052$, $\rho=0.089$, Fig. 5E). Kaplan–Meier survival curve demonstrated that high-NGEF expression+high TMB group was correlated with a worse OS, compared to the low-NGEF expression+low TMB group ($P<0.001$, Fig. 5F). The results show that the high-NGEF expression group had a higher TMB compared with the low-NGEF expression group and may thus lead to worse prognosis.

Increased NGEF expression was correlated with immune infiltration

We next investigated correlations of NGEF expression with immune infiltration. The fraction of activated memory CD4⁺ T cells ($P<0.05$), resting NK cells ($P<0.05$), and M₀ macrophage ($P<0.01$) in the high-NGEF expression group was higher than that in the low-NGEF expression group in LUAD (Fig. 6A). Furthermore, NGEF expression levels were positively associated with activated memory CD4⁺ T cells ($P=0.003$, $\rho=0.13$) and M₀ macrophage ($P<0.001$, $\rho=0.15$) (Fig. 6B–C) and were negatively associated with plasma cells ($P=0.005$, $\rho=-0.13$) and resting mast cells ($P<0.001$, $\rho=-0.16$) (Fig. 6D–E). The correlation of NGEF expression levels with levels of ICI mRNA expression was evaluated, and the results indicated that levels of ICIs, including PD1 ($P<0.001$) and PDL1 ($P<0.001$), in the high-NGEF expression group showed an obvious growth, compared to the low-NGEF expression group (Fig. 6F, H). Moreover, increased NGEF expression was correlated with higher PD1 ($P<0.001$, $\rho=0.18$) and PDL1 ($P<0.001$, $\rho=0.17$) expression (Fig. 6G, I). Therefore, the high-NGEF expression group is correlated with a dysregulated immune infiltration and may be greater sensitivity to immunotherapy.

Increased NGEF expression was correlated with chemotherapeutic sensitivity

Chemotherapy still remains an important therapeutic approach for advanced LUAD because a part of cancer patients benefits from immunotherapy according to our results and previous researches [45, 46]. Therefore, correlations of NGEF expression with chemotherapy were analyzed. The results showed that the IC50 of bortezomib, docetaxel, paclitaxel, and parthenolide was lower in the high-NGEF expression group than in the low-NGEF expression group ($P<0.001$, Fig. 7A-D), whereas the IC50 of metformin and axitinib was lower in the low-NGEF

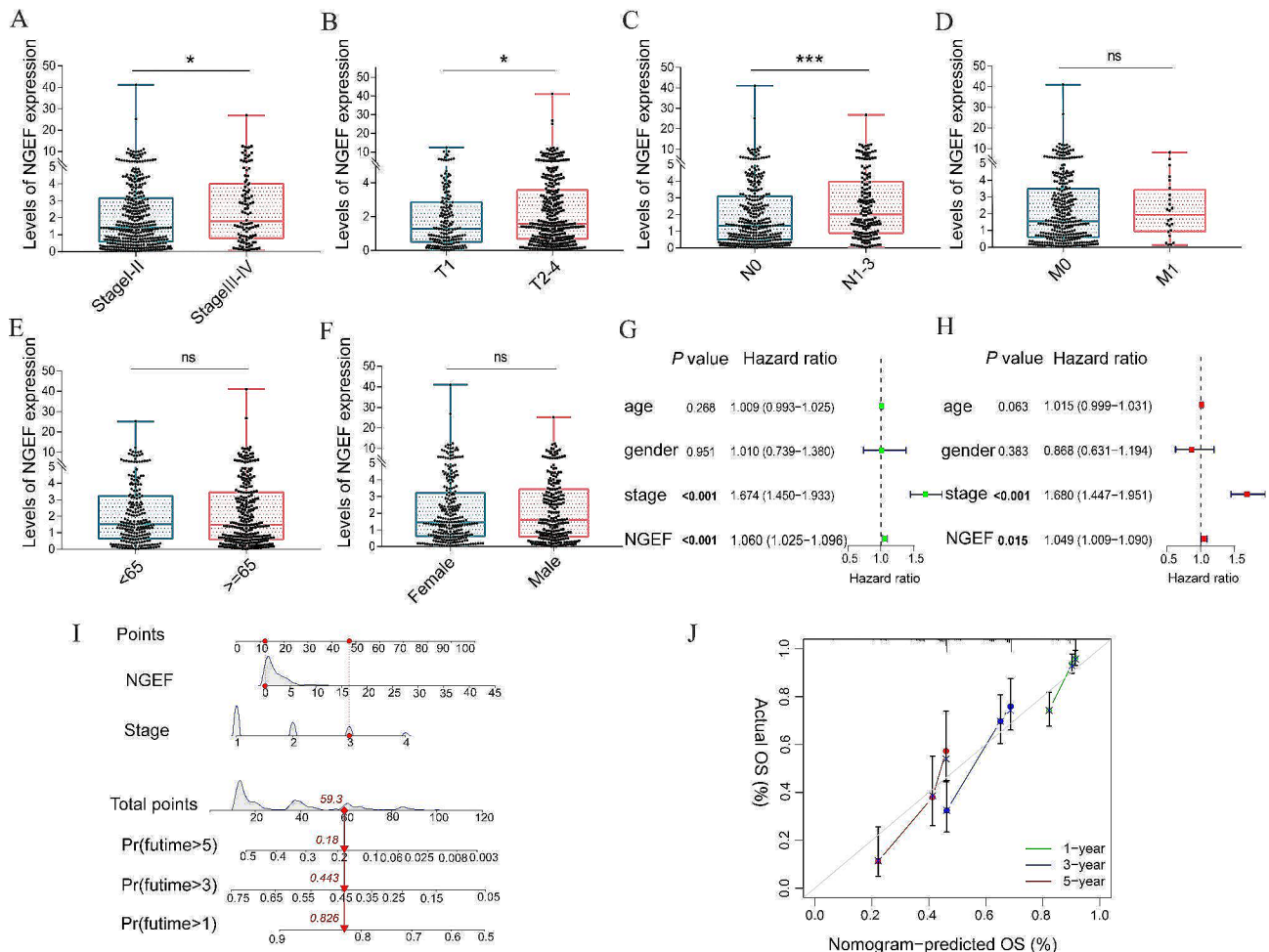


Fig. 3 Correlations of NGEF with clinical characteristics. (A) UICC stages. (B) Tumor size (≤ 3 cm and > 3 cm). (C) Lymph node metastasis (0 and ≥ 1). (D) M stages. (E) Age groups. (F) Gender groups. (G, H) Univariate and multivariate Cox regression analyses for prognosis in LUAD. (I) Nomogram to predict OS at 1, 3, and 5 years. (J) Calibration plots of the nomogram. NGEF, neuronal guanine nucleotide exchange factor; UICC, Union for International Cancer Control; OS, overall survival; ns, no significance. * $P < 0.05$, ** $P < 0.01$, *** $P < 0.001$

expression group ($P < 0.001$, Fig. 7E-F). Thus, NGEF expression may serve as reference for chemotherapeutic drug choice.

qPCR validation

The baseline information of LUAD in our center is displayed in Table 3. To verify the results of bioinformatic analysis, qPCR was carried out using lung tissues. Results reported that the relative expression of NGEF was higher in LUAD than in controls ($P = 0.007$, Fig. 8A).

Single-cell RNA sequencing analysis

To investigate the source of increased NGEF expression, single-cell RNA sequencing analysis was performed. There were 76 datasets in GEO database when tailoring to “series” and “human sapiens,” among which only 10 datasets contained more than 100 different cell samples, including GSE176021, GSE111892, GSE151531, GSE151537, GSE156138, GSE69405,

GSE127462, GSE167381, GSE111907, and GSE138734. The GSE111907 was the only dataset that met the inclusion criteria. Subsequently, 19 malignant cell samples, 20 endothelial cell samples, 17 fibroblast samples, and 20 immune cell samples from GSE111907 were included in this study. Levels of NGEF expression was significantly higher in malignant cell samples than in endothelial cell samples ($P < 0.001$), fibroblast samples ($P = 0.013$), and immune cell samples ($P < 0.001$). However, there was not a statistical significance among the endothelial cell, fibroblast, and immune cell samples (Fig. 8B).

Western blot and immunohistochemical staining

We next performed western blot and immunohistochemical staining to investigate the protein levels of NGEF between LUAD tissues and the corresponding control tissues. The results showed that the levels of NGEF-coded protein expression were higher in LUAD than in

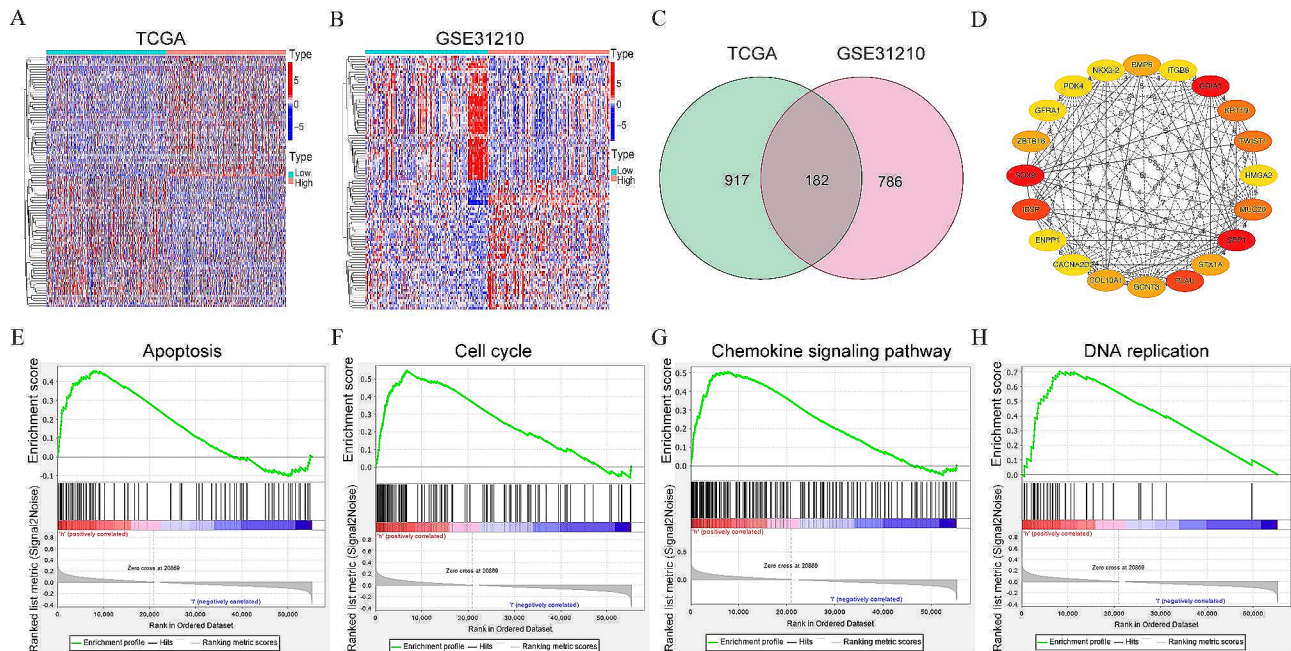


Fig. 4 DEGs, hub genes, and GSEA. **(A, B)** DEGs between the high-NGEF expression and low-NGEF expression groups in LUAD in TCGA and GSE31210. **(C)** Overlapping DEGs between TCGA and GSE31210. **(D)** Top 20 hub genes. The red color represents the most significant genes, while the yellow color represents the less significant genes. **(E)** Apoptosis. **(F)** Cell cycle. **(G)** Chemokine signaling pathway. **(H)** DNA replication. DEGs, differentially expressed genes; NGEF, neuronal guanine nucleotide exchange factor; LUAD, lung adenocarcinoma; TCGA, The Cancer Genome Atlas; GSEA, gene set enrichment analysis

Table 2 Top 20 hub genes ranked by degree in Cytoscape software

Rank	Gene ID	Log ₂ FC (TCGA)	FDR (TCGA)
1	GRIA1	-0.998	0.005
1	SOX9	0.609	< 0.001
1	SPP1	0.763	< 0.001
4	IBSP	1.618	0.001
4	PLAU	1.093	< 0.001
6	TWIST1	0.599	< 0.001
6	MUC20	0.668	< 0.001
6	KRT19	0.563	< 0.001
9	GCNT3	1.047	< 0.001
9	BMP6	-1.398	< 0.001
9	COL10A1	0.576	0.023
9	STX1A	0.519	< 0.001
9	ZBTB16	-0.958	< 0.001
14	PDK4	-0.638	0.002
14	CACNA2D2	-1.431	< 0.001
14	NKX3-2	0.881	0.001
14	GFRA1	-0.871	0.004
14	ENPP1	0.608	< 0.001
14	HMGA2	1.135	< 0.001
14	ITGB8	0.995	< 0.001

matching controls (Fig. 8C-D). Thus, we can further conclude that increased NGEF is a diagnostic biomarker for LUAD.

Discussion

In LUAD, NGEF mRNA and protein expression levels were upregulated and correlated with advanced tumor stage and worse OS. NGEF is an independent prognostic indicator for LUAD. In addition, the increased levels of NGEF expression were related to a higher fraction of activated memory CD4⁺ T cells and M₀ macrophage, elevated expression levels of ICIs, higher TMB, and better chemotherapeutic sensitivity (bortezomib, docetaxel, paclitaxel, and parthenolide).

Previous studies have demonstrated that NGEF expression is upregulated in malignant thyroid nodules [19], colorectal cancer [47] and papillary thyroid cancer [20]. Bioinformatic analyses demonstrated that NGEF expression was higher in multiple tumors. Thus, our study further confirmed that NGEF may act as an oncogene. However, the potential correlation between the NGEF and LUAD remains unclear. NGEF expression levels were upregulated in LUAD tissues in comparison with normal tissues in TCGA-LUAD and GSE31210 datasets. In addition, qPCR, IHC staining, and western blot analysis validated increased NGEF mRNA and protein levels in LUAD. Besides, AUC value of ROC curve exceeded 0.8 in both TCGA and GSE31210, showing a high diagnostic value. These findings indicate that NGEF could be a

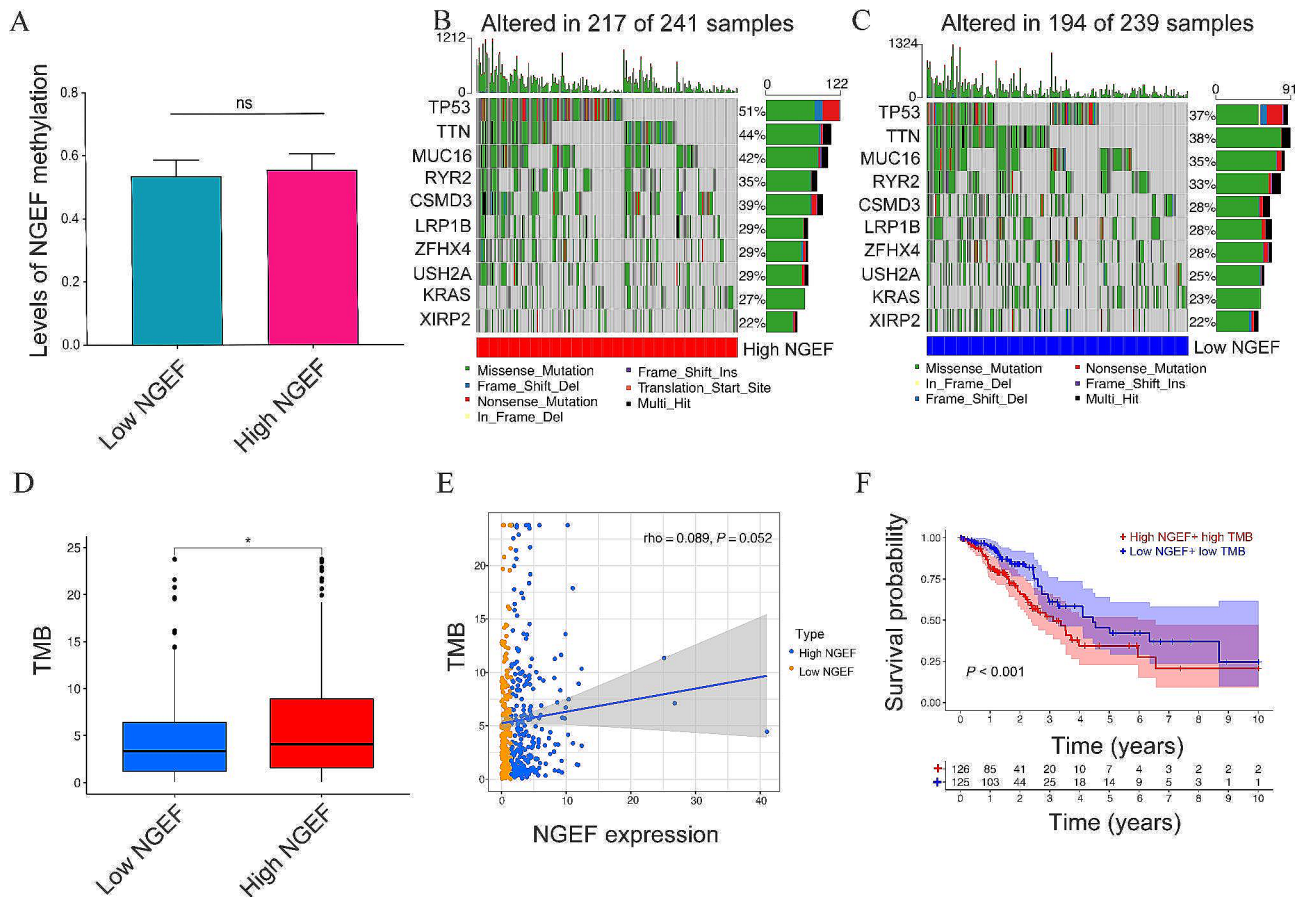


Fig. 5 Methylation and mutation analyses. **(A)** Levels of NGEF methylation between the two NGEF expression groups. **(B, C)** Top 10 mutated genes in the high- and low-NGEF expression groups. **(D, E)** Correlation of NGEF expression with TMB. **(F)** Kaplan–Meier survival analysis between the high-NGEF expression + high TMB group and low-NGEF expression + low TMB group. NGEF, neuronal guanine nucleotide exchange factor; TMB, tumor mutation burden; ns, no significance. * $P < 0.05$

potential diagnostic biomarker for LUAD. The associations of NGEF with clinical characteristics were evaluated, and the results showed that NGEF expression levels were positively correlated with the tumor size and lymph node metastasis, further corroborating that NGEF expression might be related to the disease stage and degree of malignancy of LUAD. Kaplan–Meier survival curves showed that increased NGEF expression was associated with a shorter OS, which was consistent with the previous results in papillary thyroid cancer [20]. In addition, NGEF expression was independently associated with prognosis. The constructed nomogram could predict the OS probability at 1-, 3-, and 5-year in LUAD with a good predictive value. Therefore, NGEF may serve as a prognostic biomarker for patients with LUAD.

Interactions between epidermal growth factor receptor (EGFR) and EphA2 promote tumorigenesis through the action of Ephexin1 [48]. Besides, AKT-mediated Ephexin1-Ras interaction promotes oncogenic Ras signaling and cancer cell proliferation in colorectal and lung cancer [47]. However, whether these potential

mechanisms are involved in LUAD deserves further investigation. GSEA showed that apoptosis, cell cycle, chemokine signaling, and DNA replication were the main pathways in the high-NGEF expression group of LUAD. Defects in apoptotic pathways foster malignant transformation of cells, tumor metastasis, and therapeutic resistance [49]. Besides, decrease in apoptotic activity contribute to tumorigenesis [50]. One of the crucial features on tumor is cell cycle dysregulation [51]. Disorder in cell cycle progression leads to unlimited proliferation and growth of tumor cells [52]. DNA replication may cause mutations [53], and gene mutations have enabled small cell lung cancer to be resistant to chemotherapy and have a lower OS probability [54]. Thus, NGEF may be related to the progression and prognosis of LUAD by activating these pathways. Disordered TMB showed its correlation with disease prognosis in cancer [55]. For example, TMB is a prognostic indicator for LUAD [56]. The high-NGEF expression group had a higher TMB, and the high-NGEF expression + high TMB group presented a shorter OS in the current study. Therefore, worse OS in

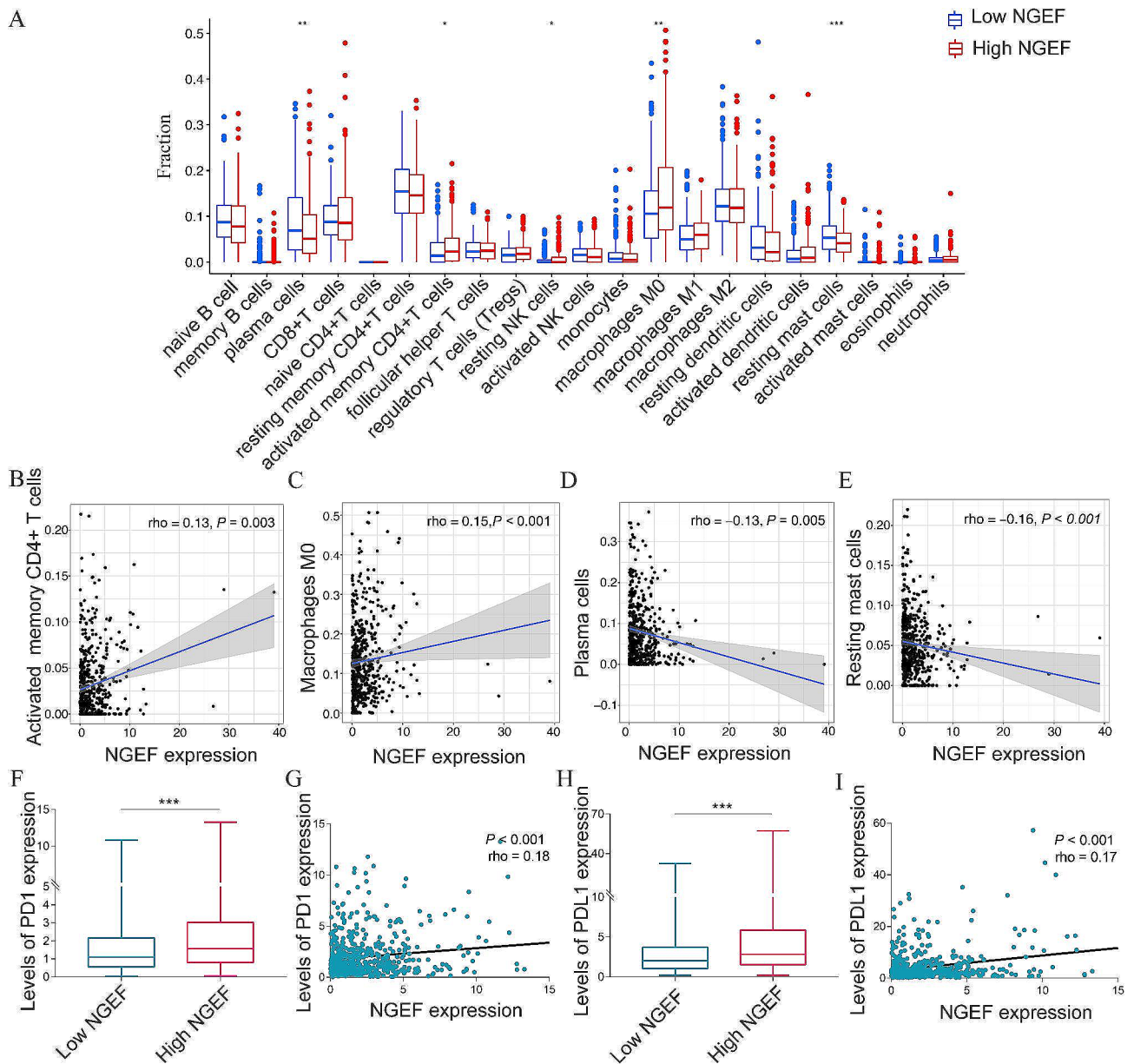


Fig. 6 Correlations of NGEF expression with immune infiltration and immune checkpoint inhibitors. **(A)** Immune infiltration. **(B)** Activated memory CD4⁺ T cells. **(C)** M₀ Macrophage. **(D)** Plasma cells. **(E)** Resting mast cells. **(F, G)** PD1. **(H, I)** PDL1. NGEF, neuronal guanine nucleotide exchange factor; PD1, programmed cell death 1; PDL1, programmed cell death 1 ligand 1. * $P < 0.05$, ** $P < 0.01$, *** $P < 0.001$

the high-NGEF expression group may be associated with increased TMB.

In the tumor microenvironment, immune cells are crucial factors for tumor progression and response on all kinds of therapy [57]. Tumor-associated macrophages (TAMs) foster disease progression and immune escape via producing various inflammatory cytokines and chemokines [58]. Higher fractions of macrophages in cancer are associated with a worse OS [59]. The previous study has showed that TAMs are generally characterized by M2-like macrophages [60], which promote angiogenesis, invasion, metastasis, and resistance to therapy [61].

However, our findings only indicated a positive correlation of NGEF expression with M₀ macrophage. Another study shows that knockdown of Circ_0001715 in M₀ macrophages suppresses LUAD cell proliferation, migration and invasion [62]. Thus, M₀ macrophages may play important role in cancer cell proliferation, migration and invasion. However, the potential mechanisms of M₀ macrophages in LUAD need to be further investigated in future studies. ICIs have been proved its antitumor immunity [63, 64]. Clinically, atezolizumab and sintilimab showed improved OS, quality of life, and a favorable safety profile in NSCLC [65, 66]. Besides, nivolumab

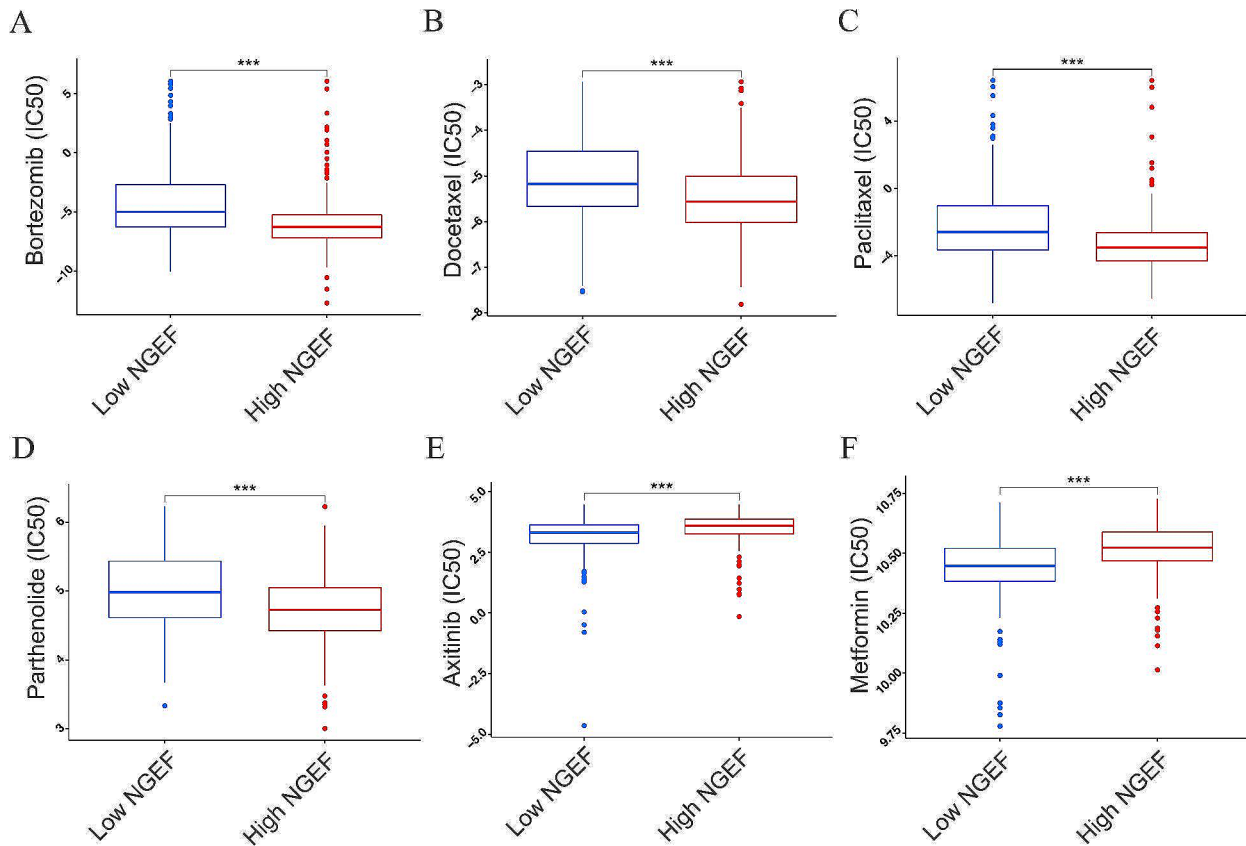


Fig. 7 IC₅₀ of six chemotherapeutic drugs. **(A)** Bortezomib. **(B)** Docetaxel. **(C)** Paclitaxel. **(D)** Parthenolide. **(E)** Axitinib. **(F)** Metformin. NGEF, neuronal guanine nucleotide exchange factor; IC₅₀, half inhibitory concentration. *** $P < 0.001$

Table 3 Clinical characteristics of 30 paired lung tissues from patients with LUAD.

Clinical characteristics	patients (30)
Age, years	70 (65–73)
Male, n (%)	24 (80.00%)
Smoking status, n (%)	21 (70.00%)
UICC stage I-II, n (%)	11 (36.67%)

plus ipilimumab showed durable long-term efficacy in advanced NSCLC [67]. However, only a subset of patients with NSCLC can clinically benefit from it [68]. Selecting the right patient for a given therapy remains a critical unmet clinical need. Our results showed that NGEF expression was positively associated with ICIs (PD1 and PDL1) levels. Thus, these results reveal that high NGEF expression may be a useful indicator for response to immunotherapy. However, the patients with the low NGEF expression may benefit less from immunotherapy; thus, chemotherapeutic sensitivity was performed to screen proper chemotherapeutic drugs for the low-NGEF expression group. Our study showed that two chemotherapeutic drugs (axitinib and metformin) were more sensitive in the low-NGEF expression group. Besides, four chemotherapeutic drugs were more sensitive in the high-NGEF expression group. Cancer patients may

benefit more from immunotherapy combined with chemotherapy compared with single immunotherapy or chemotherapy [69, 70], such as nivolumab plus ipilimumab with chemotherapy [71] and nivolumab plus chemotherapy [72, 73]. Thus, a better therapeutic strategy for high-NGEF expression group may be an immunotherapy combined with chemotherapy. Therefore, NGEF may serve as a reference for individualized therapy.

The present study highlights the following findings. First, our study reported that NGEF acts as an oncogene in several tumors and that NGEF is a diagnostic and prognostic biomarker for LUAD. Second, comprehensive and deep bioinformatic analysis was performed in the current study, including diagnostic and prognostic value; mechanism levels, such as methylation, mutation, GSEA, and immune infiltration; and therapeutic levels, such as immunotherapy and chemotherapy. Third, qPCR, IHC staining, scRNA-seq analysis, and western blot validated NGEF expression in the lung tissue. However, some limitations of our study must be noted. Although bioinformatic analyses revealed that NGEF expression was associated with immune infiltration and that apoptosis, cell cycle, chemokine signaling pathway, and DNA replication were the main pathways, further studies are

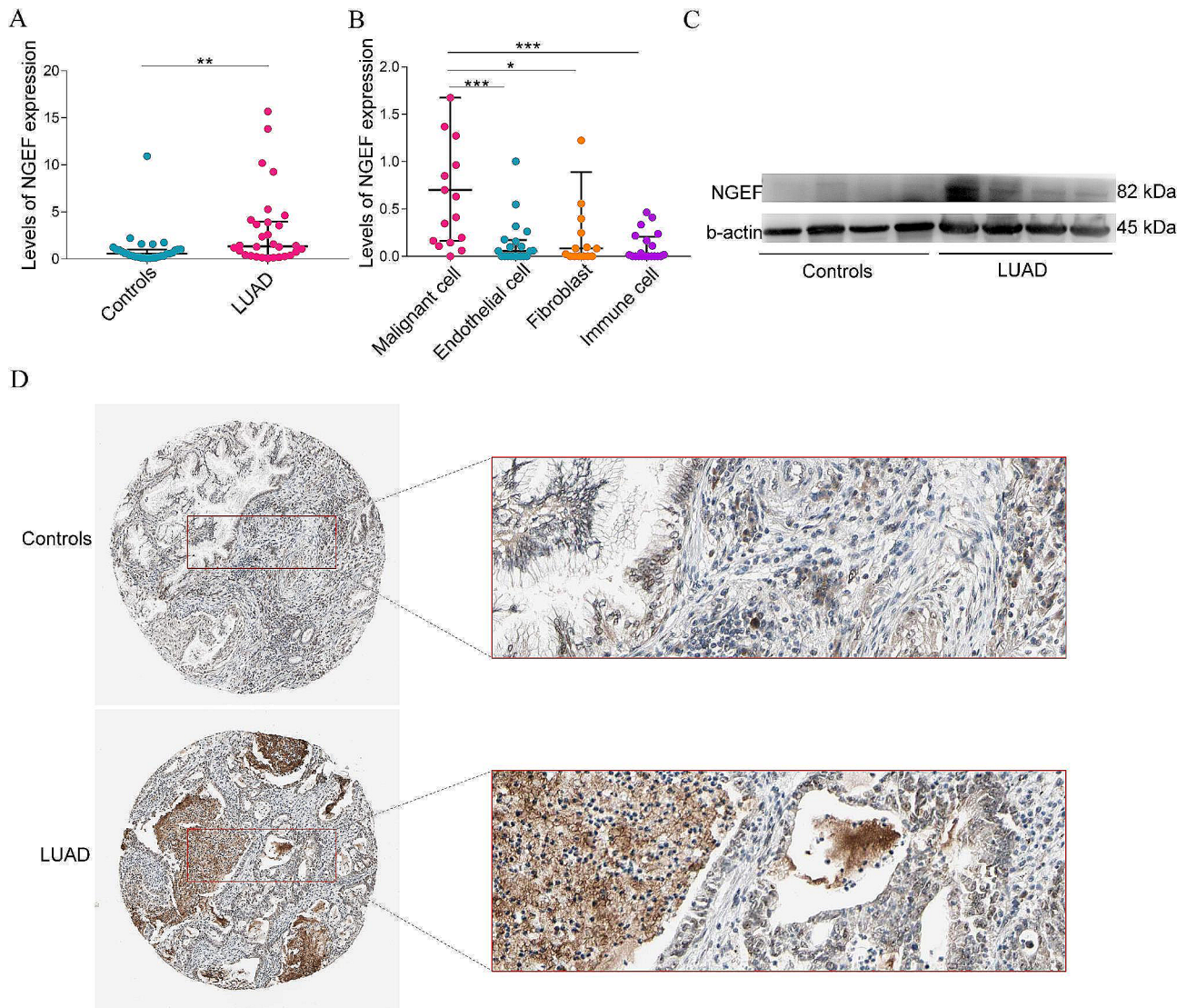


Fig. 8 Validation of NGEF in LUAD. **(A)** Quantitative PCR validation of NGEF expression. **(B)** Single-cell RNA sequencing-based analysis of NGEF expression. **(C)** Western blot analysis of NGEF expression. **(D)** Immunohistochemical data of NGEF from The Human Protein Atlas. NGEF, neuronal guanine nucleotide exchange factor; LUAD, lung adenocarcinoma. * $P < 0.05$, ** $P < 0.01$, *** $P < 0.001$

warranted to investigate the specific role of NGEF in the tumor microenvironment and related pathways. Additionally, the mechanism by which NGEF is involved in tumor migration, invasion, and metastasis needs to be confirmed in vivo and in vitro.

Conclusion

Using bioinformatic analysis, we systematically analyzed the expression patterns and prognostic and therapeutic value of NGEF in patients with LUAD from various databases. Our results indicate that the high NGEF expression has an advanced tumor stage and worse OS and that NGEF is an independent prognostic factor for LUAD. Moreover, increased NGEF expression was related to dysregulated immune infiltration, elevated ICI levels,

higher TMB, and better sensitivity to four chemotherapeutic drugs (bortezomib, docetaxel, paclitaxel, and parthenolide). However, the low NGEF expression was more sensitive to two chemotherapeutic drugs. These findings reveal that NGEF may be a potential diagnostic and prognostic biomarker and therapeutic target for immunotherapy and chemotherapy in LUAD.

Supplementary Information

The online version contains supplementary material available at <https://doi.org/10.1186/s12890-024-03046-1>.

Supplementary Material 1

Acknowledgements

Not applicable.

Author contributions

Yan-qiu He collected data, performed qPCR and western blot, and drafted the manuscript. Tao Zhang analyzed data and revised the manuscript. Ti-wei Miao, Qi Zhu, Jie Liu, and Fang-ying Chen collected and analyzed data. Jie Yin and Hong-ping Zeng revised the manuscript and edited the language. Qian Ding and Mei Yang collected data and revised manuscript. Xin Chen designed the experiment and revised the manuscript.

Funding

This research was supported by Sichuan Provincial Administration of Traditional Chinese Medicine [2021MS462] and Key R&D Program of Zigong Science and Technology Bureau [2021YX01].

Data availability

The datasets used in this study are available from the GEPIA2 database (<http://gepia2.cancer-pku.cn/#index>), TCGA database (<https://portal.gdc.cancer.gov/>), GEO database (<https://www.ncbi.nlm.nih.gov/gds/>), the Human Protein Atlas database (<https://www.proteinatlas.org/>).

Declarations**Ethics approval and consent to participate**

This study was approved by the Clinical Trial and Biomedical Ethics Committee of Zigong First People's Hospital (No.2021-24) and was conducted in accordance with the principles of Declaration of Helsinki. All patients volunteered to attend the study and signed an informed consent.

Consent for publication

Not applicable.

Competing interests

The authors declare no competing interests.

Author details

¹Department of Integrated Traditional Chinese and Western Medicine, Zigong First People's Hospital, Zigong, China

²Department of Intensive Care Unit, Chongqing General Hospital, University of Chinese Academy of Sciences, Chongqing, China

³School of Automation & Information Engineering, Sichuan university of Science & Engineering, Zigong, China

⁴Department of Tuberculosis, The Third People's Hospital of Tibet Autonomous Region, Lhasa, China

Received: 16 October 2023 / Accepted: 6 May 2024

Published online: 19 May 2024

References

- Sung H, Ferlay J, Siegel RL, Laversanne M, Soerjomataram I, Jemal A, et al. Global Cancer statistics 2020: GLOBOCAN estimates of incidence and Mortality Worldwide for 36 cancers in 185 countries. *CA Cancer J Clin*. 2021;71(3):209–49. <https://doi.org/10.3322/caac.21660>.
- AbdulJabbar K, Raza SEA, Rosenthal R, Jamal-Hanjani M, Veeriah S, Akrar A, et al. Geospatial immune variability illuminates differential evolution of lung adenocarcinoma. *Nat Med*. 2020;26(7):1054–62. <https://doi.org/10.1038/s41591-020-0900-x>.
- Liu X, Xiang D, Xu C, Chai R. EIF3m promotes the malignant phenotype of lung adenocarcinoma by the up-regulation of oncogene CAPRIN1. *Am J Cancer Res*. 2021;11(3):979–96.
- Zhang Y, Ma X, Shen X, Wang S, Li Y, Hu H, et al. Surgery for pre- and minimally invasive lung adenocarcinoma. *J Thorac Cardiovasc Surg*. 2020. <https://doi.org/10.1016/j.jtcvs.2020.11.151>.
- Baratella E, Cernic S, Minelli P, Furlan G, Crimi F, Rocco S, et al. Accuracy of CT-Guided core-needle biopsy in diagnosis of thoracic lesions suspicious for primitive malignancy of the lung: a five-year retrospective analysis. *Tomography*. 2022;8(6):2828–38. <https://doi.org/10.3390/tomography8060236>.
- Allemani C, Matsuda T, Di Carlo V, Harewood R, Matz M, Nikšić M, et al. Global surveillance of trends in cancer survival 2000–14 (CONCORD-3): analysis of individual records for 37 513 025 patients diagnosed with one of 18 cancers from 322 population-based registries in 71 countries. *Lancet*. 2018;391(10125):1023–75. [https://doi.org/10.1016/s0140-6736\(17\)33326-3](https://doi.org/10.1016/s0140-6736(17)33326-3).
- Stella GM, Luisetti M, Pozzi E, Comoglio PM. Oncogenes in non-small-cell lung cancer: emerging connections and novel therapeutic dynamics. *Lancet Respir Med*. 2013;1(3):251–61. [https://doi.org/10.1016/s2213-2600\(13\)70009-2](https://doi.org/10.1016/s2213-2600(13)70009-2).
- Li Z, Feng Y, Li P, Wang S, Liu X, Xia S. CD1B is a potential Prognostic Biomarker Associated with Tumor Mutation Burden and promotes Antitumor Immunity in Lung Adenocarcinoma. *Int J Gen Med*. 2022;15:3809–26. <https://doi.org/10.2147/ijgm.s352851>.
- Zhong A, Chen T, Zhou T, Zhang Z, Shi M. TPD52L2 is a prognostic biomarker and correlated with Immune Infiltration in Lung Adenocarcinoma. *Front Pharmacol*. 2021;12:728420. <https://doi.org/10.3389/fphar.2021.728420>.
- Sun M, Wang T, Zhu Y, Zhang Y, Zhu L, Li X. The High Expression of Minichromosome Maintenance Complex Component 5 Is an Adverse Prognostic Factor in Lung Adenocarcinoma. *Biomed Res Int*. 2022. 2022: 4338793. <https://doi.org/10.1155/2022/4338793>.
- Wang D, Jia Y, Zheng W, Li C, Cui W. Overexpression of eIF3D in lung adenocarcinoma is a new independent prognostic marker of poor survival. *Dis Markers*. 2019;2019(6019637). <https://doi.org/10.1155/2019/6019637>.
- Zhou J, Lin H, Ni Z, Luo R, Yang D, Feng M, et al. Expression of PD-L1 through evolution phase from pre-invasive to invasive lung adenocarcinoma. *BMC Pulm Med*. 2023;23(1):18. <https://doi.org/10.1186/s12890-023-02310-0>.
- Liang KH, Luo YH, Wang ML, Chiou SH, Chen YM, Hsu HS. A multiomic investigation of lung adenocarcinoma molecular subtypes. *J Chin Med Assoc*. 2024;87(1):33–9. <https://doi.org/10.1097/jcma.0000000000001029>.
- Shamah SM, Lin MZ, Goldberg JL, Estrach S, Sahin M, Hu L, et al. EphA receptors regulate growth cone dynamics through the novel guanine nucleotide exchange factor ephexin. *Cell*. 2001;105(2):233–44. [https://doi.org/10.1016/s0092-8674\(01\)00314-2](https://doi.org/10.1016/s0092-8674(01)00314-2).
- Sahin M, Greer PL, Lin MZ, Poucher H, Eberhart J, Schmidt S, et al. Eph-dependent tyrosine phosphorylation of ephexin1 modulates growth cone collapse. *Neuron*. 2005;46(2):191–204. <https://doi.org/10.1016/j.neuron.2005.01.030>.
- Rodrigues NR, Theodosiou AM, Nesbit MA, Campbell L, Tandle AT, Saranath D, et al. Characterization of Ngef, a novel member of the Dbl family of genes expressed predominantly in the caudate nucleus. *Genomics*. 2000;65(1):53–61. <https://doi.org/10.1006/geno.2000.6138>.
- Guo L, Frost MR, Siegwart Jr JT, Norton TT. Scleral gene expression during recovery from myopia compared with expression during myopia development in tree shrew. *Mol Vis*. 2014;20:1643–59.
- Kim HJ, Park JH, Lee S, Son HY, Hwang J, Chae J, et al. A common variant of NGEF is Associated with Abdominal Visceral Fat in Korean men. *PLoS ONE*. 2015;10(9):e0137564. <https://doi.org/10.1371/journal.pone.0137564>.
- Wang QX, Chen ED, Cai YF, Li Q, Jin YX, Jin WX, et al. A panel of four genes accurately differentiates benign from malignant thyroid nodules. *J Exp Clin Cancer Res*. 2016;35(1):169. <https://doi.org/10.1186/s13046-016-0447-3>.
- Han Y, Yu X, Yin Y, Lv Z, Jia C, Liao Y, et al. Identification of potential BRAF inhibitor joint therapy targets in PTC based on WGCAN and DCGA. *J Cancer*. 2021;12(6):1779–91. <https://doi.org/10.7150/jca.51551>.
- Zheng R, Zhang S, Zeng H, et al. Cancer incidence and mortality in China. *J Natl Cancer Cent*. 2016. <https://doi.org/10.1016/j.jncc.2022.02.002>.
- Li C, Tang Z, Zhang W, Ye Z, Liu F. GEPIA2021: integrating multiple deconvolution-based analysis into GEPIA. *Nucleic Acids Res*. 2021;49(W1):W242–6. <https://doi.org/10.1093/nar/gkab418>.
- Weinstein JN, Collisson EA, Mills GB, Shaw KR, Ozenberger BA, Ellrott K, et al. The Cancer Genome Atlas Pan-Cancer analysis project. *Nat Genet*. 2013;45(10):1113–20. <https://doi.org/10.1038/ng.2764>.
- Comprehensive molecular profiling of lung adenocarcinoma. *Nature*. 2014. 511(7511): 543–50. <https://doi.org/10.1038/nature13385>.
- Okayama H, Kohno T, Ishii Y, Shimada Y, Shiraishi K, Iwakawa R, et al. Identification of genes upregulated in ALK-positive and EGFR/KRAS/ALK-negative lung adenocarcinomas. *Cancer Res*. 2012;72(1):100–11. <https://doi.org/10.1158/0008-5472.can-11-1403>.
- Edgar R, Domrachev M, Lash AE. Gene expression Omnibus: NCB1 gene expression and hybridization array data repository. *Nucleic Acids Res*. 2002;30(1):207–10. <https://doi.org/10.1093/nar/30.1.207>.
- Huang L, Lin W, Xie D, Yu Y, Cao H, Liao G, et al. Development and validation of a preoperative CT-based radiomic nomogram to predict pathology invasiveness in patients with a solitary pulmonary nodule: a machine learning

- approach, multicenter, diagnostic study. *Eur Radiol.* 2022;32(3):1983–96. <https://doi.org/10.1007/s00330-021-08268-z>.
28. Luo LM, Wang Y, Lin PX, Su CH, Huang BT. The clinical outcomes, prognostic factors and Nomogram models for primary lung Cancer patients treated with stereotactic body Radiation Therapy. *Front Oncol.* 2022;12:863502. <https://doi.org/10.3389/fonc.2022.863502>.
 29. Szklarczyk D, Gable AL, Lyon D, Junge A, Wyder S, Huerta-Cepas J, et al. STRING v11: protein-protein association networks with increased coverage, supporting functional discovery in genome-wide experimental datasets. *Nucleic Acids Res.* 2019;47(D1):D607–13. <https://doi.org/10.1093/nar/gky1131>.
 30. Subramanian A, Tamayo P, Mootha VK, Mukherjee S, Ebert BL, Gillette MA, et al. Gene set enrichment analysis: a knowledge-based approach for interpreting genome-wide expression profiles. *Proc Natl Acad Sci U S A.* 2005;102(43):15545–50. <https://doi.org/10.1073/pnas.0506580102>.
 31. Yin YP, Shi WH, Deng K, Liu XL, Li H, Lv XT, et al. Combinations of proteasome inhibitors with obatoclax are effective for small cell lung cancer. *Acta Pharmacol Sin.* 2021;42(8):1298–310. <https://doi.org/10.1038/s41401-020-00544-w>.
 32. Wang WH, Zhan JM, Tang YL, Zhou N, Liu WY, Jiang DW. miR-466 contributes to the enhanced Antitumor Effect of Bortezomib on Non-small-cell Lung Cancer by inhibiting CCND1. *Chemotherapy.* 2022;1–12. <https://doi.org/10.1159/000518936>.
 33. Xiao D, Hu X, Zhang J. Tumour targeted polymer nanoparticles co-loaded with docetaxel and siCCAT2 for combination therapy of lung cancer. *J Drug Target.* 2022; 1–10. <https://doi.org/10.1080/1061186x.2021.2016773>.
 34. Feng X, Xiong X, Ma S. Docetaxel-Loaded Novel Nano-platform for synergistic therapy of Non-small Cell Lung Cancer. *Front Pharmacol.* 2022;13:832725. <https://doi.org/10.3389/fphar.2022.832725>.
 35. Ren S, Chen J, Xu X, Jiang T, Cheng Y, Chen G, et al. Camrelizumab Plus Carboplatin and Paclitaxel as First-Line treatment for advanced squamous NSCLC (Camel-Sq): a phase 3 trial. *J Thorac Oncol.* 2022;17(4):544–57. <https://doi.org/10.1016/j.jtho.2021.11.018>.
 36. Duan L, Perez RE, Calhoun S, Maki CG. Inhibitors of Jumonji C domain-containing histone lysine demethylases overcome cisplatin and paclitaxel resistance in non-small cell lung cancer through APC/Cdh1-dependent degradation of CtIP and PAF15. *Cancer Biol Ther.* 2022;23(1):65–75. <https://doi.org/10.1080/15384047.2021.2020060>.
 37. Li X, Huang R, Li M, Zhu Z, Chen Z, Cui L, et al. Parthenolide inhibits the growth of non-small cell lung cancer by targeting epidermal growth factor receptor. *Cancer Cell Int.* 2020;20(1):561. <https://doi.org/10.1186/s12935-020-01658-1>.
 38. Sun L, Yuan W, Wen G, Yu B, Xu F, Gan X, et al. Parthenolide inhibits human lung cancer cell growth by modulating the IGF-1R/PI3K/Akt signaling pathway. *Oncol Rep.* 2020;44(3):1184–93. <https://doi.org/10.3892/or.2020.7649>.
 39. Solomon B, Callejo A, Bar J, Berchem G, Bazhenova L, Saintigny P, et al. A WIN Consortium phase I study exploring avelumab, palbociclib, and axitinib in advanced non-small cell lung cancer. *Cancer Med.* 2022. <https://doi.org/10.1002/cam4.4635>.
 40. Wang M, Wang X, Li Y, Xiao Q, Cui XH, Xiao GD, et al. Nutlin-3-Induced sensitization of Non-small Cell Lung Cancer Stem cells to Axitinib-Induced apoptosis through repression of Akt1/Wnt signaling. *Oncol Res.* 2019;27(9):987–95. <https://doi.org/10.3727/096504018x15424918479652>.
 41. Bondarenko IM, Ingrassio A, Bycott P, Kim S, Cebotaru CL. Phase II study of axitinib with doublet chemotherapy in patients with advanced squamous non-small-cell lung cancer. *BMC Cancer.* 2015;15:339. <https://doi.org/10.1186/s12885-015-1350-6>.
 42. Chen N, Zhou YS, Wang LC, Huang JB. Advances in metformin-based metabolic therapy for non-small cell lung cancer (review). *Oncol Rep.* 2022;47(3). <https://doi.org/10.3892/or.2022.8266>.
 43. Arrieta O, Zatarain-Barrón ZL, Turcott JG, Barrón F, Yendamuri S, Cardona AF, et al. Association of BMI with Benefit of Metformin plus epidermal growth factor receptor-tyrosine kinase inhibitors in patients with Advanced Lung Adenocarcinoma: a secondary analysis of a phase 2 Randomized Clinical Trial. *JAMA Oncol.* 2022;8(3):477–9. <https://doi.org/10.1001/jamaoncol.2021.7015>.
 44. Uhlén M, Fagerberg L, Hallström BM, Lindskog C, Oksvold P, Mardinoglu A, et al. Proteomics. Tissue-based map of the human proteome. *Science.* 2015;347(6220):1260419. <https://doi.org/10.1126/science.1260419>.
 45. Passaro A, Brahmeh J, Antonia S, Mok T, Peters S. Managing resistance to Immune checkpoint inhibitors in Lung Cancer: treatment and novel strategies. *J Clin Oncol.* 2022;40(6):598–610. <https://doi.org/10.1200/jco.2021.01845>.
 46. He D, Wang D, Lu P, Yang N, Xue Z, Zhu X, et al. Single-cell RNA sequencing reveals heterogeneous tumor and immune cell populations in early-stage lung adenocarcinomas harboring EGFR mutations. *Oncogene.* 2021;40(2):355–68. <https://doi.org/10.1038/s41388-020-01528-0>.
 47. Kim J, Jeon YJ, Lim SC, Ryu J, Lee JH, Chang IY, et al. Akt-mediated Ephexin-1-Ras interaction promotes oncogenic ras signaling and colorectal and lung cancer cell proliferation. *Cell Death Dis.* 2021;12(11):1013. <https://doi.org/10.1038/s41419-021-04332-0>.
 48. Kim J, Chang IY, You HJ. Interactions between EGFR and EphA2 promote tumorigenesis through the action of Ephexin1. *Cell Death Dis.* 2022;13(6):528. <https://doi.org/10.1038/s41419-022-04984-6>.
 49. Ghafouri-Fard S, Aghabalazade A, Shoorai H, Majidpoor J, Taheri M, Mokhtari M. The impact of lncRNAs and miRNAs on apoptosis in Lung Cancer. *Front Oncol.* 2021;11:714795. <https://doi.org/10.3389/fonc.2021.714795>.
 50. Diepstraten ST, Anderson MA, Czabotar PE, Lessene G, Strasser A, Kelly GL. The manipulation of apoptosis for cancer therapy using BH3-mimetic drugs. *Nat Rev Cancer.* 2022;22(1):45–64. <https://doi.org/10.1038/s41568-021-00407-4>.
 51. Malumbres M, Barbacid M. Cell cycle, CDKs and cancer: a changing paradigm. *Nat Rev Cancer.* 2009;9(3):153–66. <https://doi.org/10.1038/nrc2602>.
 52. Mohammadi M, Bagheri L, Badreldin A, Fatehi P, Pakzad L, Surtres Z, et al. Biological effects of Gyrophoric Acid and other Lichen Derived metabolites, on cell proliferation, apoptosis and cell signaling pathways. *Chem Biol Interact.* 2022;351:109768. <https://doi.org/10.1016/j.cbi.2021.109768>.
 53. Basu AK. DNA damage, mutagenesis and Cancer. *Int J Mol Sci.* 2018;19(4). <https://doi.org/10.3390/ijms19040970>.
 54. Kandath C, McLellan MD, Vandin F, Ye K, Niu B, Lu C, et al. Mutational landscape and significance across 12 major cancer types. *Nature.* 2013;502(7471):333–9. <https://doi.org/10.1038/nature12634>.
 55. Klemperer SJ, Fabrizio D, Bane S, Reinhart M, Peoples T, Ali SM, et al. Tumor Mutational Burden as a predictive biomarker for response to Immune Checkpoint inhibitors: a review of current evidence. *Oncologist.* 2020;25(1):e147–59. <https://doi.org/10.1634/theoncologist.2019-0244>.
 56. Zhao Z, He B, Cai Q, Zhang P, Peng X, Zhang Y, et al. Combination of tumor mutation burden and immune infiltrates for the prognosis of lung adenocarcinoma. *Int Immunopharmacol.* 2021;98:107807. <https://doi.org/10.1016/j.intimp.2021.107807>.
 57. Suzuki J, Aokage K, Neri S, Sakai T, Hashimoto H, Su Y, et al. Relationship between podoplanin-expressing cancer-associated fibroblasts and the immune microenvironment of early lung squamous cell carcinoma. *Lung Cancer.* 2021;153:1–10. <https://doi.org/10.1016/j.lungcan.2020.12.020>.
 58. Cully M, Cancer. Re-educating tumour-associated macrophages with nanoparticles. *Nat Rev Drug Discov.* 2018;17(7):468. <https://doi.org/10.1038/nrd.2018.102>.
 59. Bense RD, Sotiriou C, Piccart-Gebhart MJ, Haanen J, van Vugt M, de Vries EGE, et al. Relevance of Tumor-infiltrating Immune Cell composition and functionality for disease outcome in breast Cancer. *J Natl Cancer Inst.* 2017;109(1). <https://doi.org/10.1093/jnci/djw192>.
 60. Zheng X, Weigert A, Reu S, Guenther S, Mansouri S, Bassaly B, et al. Spatial density and distribution of Tumor-Associated macrophages Predict Survival in Non-small Cell Lung Carcinoma. *Cancer Res.* 2020;80(20):4414–25. <https://doi.org/10.1158/0008-5472.can-20-0069>.
 61. Yin M, Li X, Tan S, Zhou HJ, Ji W, Bellone S, et al. Tumor-associated macrophages drive spheroid formation during early transcoelomic metastasis of ovarian cancer. *J Clin Invest.* 2016;126(11):4157–73. <https://doi.org/10.1172/jci87252>.
 62. Chen M, Cao C, Ma J. Tumor-related exosomal circ_0001715 promotes lung adenocarcinoma cell proliferation and metastasis via enhancing M2 macrophage polarization by regulating triggering receptor expressed on myeloid cells-2. *Thorac Cancer.* 2024;15(3):227–38. <https://doi.org/10.1111/1759-7714.15182>.
 63. Cai X, Zhan H, Ye Y, Yang J, Zhang M, Li J, et al. Current progress and future perspectives of Immune Checkpoint in Cancer and Infectious diseases. *Front Genet.* 2021;12:785153. <https://doi.org/10.3389/fgene.2021.785153>.
 64. Alemohammad H, Najafzadeh B, Asadzadeh Z, Baghbanzadeh A, Ghorbaninezhad F, Najafzadeh A, et al. The importance of immune checkpoints in immune monitoring: a future paradigm shift in the treatment of cancer. *Biomed Pharmacother.* 2021;146:112516. <https://doi.org/10.1016/j.biopha.2021.112516>.
 65. Lee SM, Schulz C, Prabhaskar K, Kowalski D, Szczesna A, Han B, et al. First-line atezolizumab monotherapy versus single-agent chemotherapy in patients with non-small-cell lung cancer ineligible for treatment with a platinum-containing regimen (IPSOS): a phase 3, global, multicentre, open-label, randomised controlled study. *Lancet.* 2023;402(10400):451–63. [https://doi.org/10.1016/s0140-6736\(23\)00774-2](https://doi.org/10.1016/s0140-6736(23)00774-2).

66. Zhang F, Guo W, Zhou B, Wang S, Li N, Qiu B, et al. Three-year Follow-Up of Neoadjuvant programmed cell death Protein-1 inhibitor (Sintilimab) in NSCLC. *J Thorac Oncol.* 2022;17(7):909–20. <https://doi.org/10.1016/j.jtho.2022.04.012>.
67. Paz-Ares LG, Ramalingam SS, Ciuleanu TE, Lee JS, Urban L, Caro RB, et al. First-line Nivolumab Plus Ipilimumab in Advanced NSCLC: 4-Year outcomes from the Randomized, Open-Label, phase 3 CheckMate 227 part 1 trial. *J Thorac Oncol.* 2022;17(2):289–308. <https://doi.org/10.1016/j.jtho.2021.09.010>.
68. Rodríguez-Abreu D, Powell SF, Hochmair MJ, Gadgeel S, Esteban E, Felip E, et al. Pemetrexed plus platinum with or without pembrolizumab in patients with previously untreated metastatic nonsquamous NSCLC: protocol-specified final analysis from KEYNOTE-189. *Ann Oncol.* 2021;32(7):881–95. <https://doi.org/10.1016/j.annonc.2021.04.008>.
69. Chen S, Yang Y, Wang R, Fang J. Neoadjuvant PD-1/PD-L1 inhibitors combined with chemotherapy had a higher ORR than mono-immunotherapy in untreated HNSCC: Meta-analysis. *Oral Oncol.* 2023;145:106479. <https://doi.org/10.1016/j.oraloncology.2023.106479>.
70. Zhang Z, Wang D, Zhang J, Ruan Y, Zhao L, Yang L, et al. Comparison of the effectiveness of chemotherapy combined with immunotherapy and chemotherapy alone in advanced biliary tract cancer and construction of the nomogram for survival prediction based on the inflammatory index and controlling nutritional status score. *Cancer Immunol Immunother.* 2023. <https://doi.org/10.1007/s00262-023-03513-4>.
71. Carbone DP, Ciuleanu TE, Schenker M, Cobo M, Bordenave S, Juan-Vidal O, et al. Four-year clinical update and treatment switching-adjusted outcomes with first-line nivolumab plus ipilimumab with chemotherapy for metastatic non-small cell lung cancer in the CheckMate 9LA randomized trial. *J Immunother Cancer.* 2024;12(2). <https://doi.org/10.1136/jitc-2023-008189>.
72. Provencio M, Nadal E, González-Larriba JL, Martínez-Martí A, Bernabé R, Bosch-Barrera J, et al. Perioperative Nivolumab and Chemotherapy in Stage III Non-small-cell Lung Cancer. *N Engl J Med.* 2023;389(6):504–13. <https://doi.org/10.1056/NEJMoa2215530>.
73. Forde PM, Spicer J, Lu S, Provencio M, Mitsudomi T, Awad MM, et al. Neoadjuvant Nivolumab plus Chemotherapy in Resectable Lung Cancer. *N Engl J Med.* 2022;386(21):1973–85. <https://doi.org/10.1056/NEJMoa2202170>.

Publisher's Note

Springer Nature remains neutral with regard to jurisdictional claims in published maps and institutional affiliations.